Case Studies in Thermal Engineering 9 (2017) 1–13

Contents lists available at ScienceDirect

Case Studies in Thermal Engineering

journal homepage: www.elsevier.com/locate/csite

A comparative thermodynamic analysis of ORC and Kalina cycles for waste heat recovery: A case study for CGAM cogeneration system

Arash Nemati, Hossein Nami*, Faramarz Ranjbar, Mortaza Yari

Faculty of Mechanical Engineering, University of Tabriz, 29th Bahman Blvd., Tabriz, Iran

ARTICLE INFO

Keywords:
CGAM cogeneration system
Waste heat recovery
ORC
Kalina
Energy and exergy
TSP

ABSTRACT

A thermodynamic modeling and optimization is carried out to compare the advantages and disadvantages of organic Rankine cycle (ORC) and Kalina cycle (KC) as a bottoming cycle for waste heat recovery from CGAM cogeneration system. Thermodynamic models for combined CGAM/ORC and CGAM/KC systems are performed and the effects of some decision variables on the energy and exergy efficiency and turbine size parameter of the combined systems are investigated. Solving simulation equations and optimization process have been done using direct search method by EES software. It is observed that at the optimum pressure ratio of air compressor, produced power of bottoming cycles has minimum values. Also, evaporator pressure optimizes the performance of cycle, but this optimum pressure level in ORC (11 bar) is much lower than that of Kalina (46 bar). In addition, ORC's simpler configuration, higher net produced power and superheated turbine outlet flow, which leads to a reliable performance for turbine, are other advantages of ORC. Kalina turbine size parameter is lower than that of the ORC which is a positive aspect of Kalina cycle. However, by a comprehensive comparison between Kalina and ORC, it is concluded that the ORC has significant privileges for waste heat recovery in this case.

1. Introduction

General population growth with economic development is leading to increasing energy consumption [1]. Multi-generation systems such as combined heat and power generation (CHP) are attractive. Among the cogeneration systems, gas turbine cogeneration is a well-known system which uses the hot gases leaving the gas turbine for producing saturated steam as a by-product [2–4]. One of the well-known proposed cogeneration systems, is CGAM (which was named after the first initials of the participating researchers including C. Frangopoulos, G. Tsatsaronis, A Valero and M. von Spakovsky) [3–8], which is a cogeneration plant producing 30 MW power and 14 kg/s of saturated steam. CGAM consists of a high temperature gas turbine and an air preheater to use a part of thermal energy of the hot gases leaving the gas turbine as well as a heat recovery steam generator in which the saturated steam is produced [5]. Global warming, splitting of the ozone layer and other environmental problems lead to the energy policy consideration. In addition, increasing the electricity price up to a rate of 12% annually motivates the use of waste heat and renewable

Abbreviations: AC, Air compressor; AB, Absorber; AP, Air preheater; AWT, Ammonia water turbine; CC, Combustion chamber; COND, Condenser; Eva, Evaporator; GT, Gas turbine; G, Genarator; HRSG, Heat recovery steam generator; ORCT, Organic Rankine cycle turbine; P, Pump; REG, Regenerator; SEP, Separator; V, Valve

* Corresponding author.
E-mail address: h.nami@tabrizu.ac.ir (H. Nami).

http://dx.doi.org/10.1016/j.csite.2016.11.003
Received 24 July 2016; Received in revised form 26 September 2016; Accepted 5 November 2016
Available online 18 November 2016

Nomenclature

$\dot{E}_i$	Exergy rate [kW]
$\dot{E}_D$	Exergy destruction rate [kW]
$\dot{E}_F$	Fuel exergy rate [kW]
$\dot{E}_{in}$	Entrance Exergy rate [kW]
$\dot{E}_P$	Product Exergy rate [kW]
e_i	Specific thermo mechanical flow exergy at state i [kJ/kmol]
e_{ch}	Specific chemical exergy [kJ/kmol]
e_{ph}	Specific physical exergy [kJ/kmol]
h	Specific enthalpy [kJ/kmol]
LHV	Lower heating value [kJ/kmol]
$\dot{n}$	Molar rate [kmol/s]
P_i	Pressure at state i [bar]
$\dot{Q}$	Heat transfer rate [kW]
r_p	Pressure ratio [Dimensionless]
$\overline{R}$	Universal gas constant [kJ/kmol K]
s	Specific entropy [kJ/kmol K]
T_i	Temperature at state i [K]
$\dot{W}$	Produced or consumed power by components [kW]

Greek letters

ε	Exergy efficiency [%]
$\eta_{C,isen}$	Isentropic efficiency of compressor [%]
$\eta_{T,isen}$	Isentropic efficiency of turbine [%]
$\eta_{P,isen}$	Isentropic efficiency of pump [%]
η	Energy efficiency [%]

Subscripts

0	Reference environment state
D	Destruction
env	Environmental
F	Fuel
in	Input
i	State point
k	k'th component
l	Loss
out	Outlet
P	Product
q	Heat transfer
w	Power

sources for power generation [9,10]. Possible solutions may be the use of organic Rankine cycle (ORC), Kalina cycle (KC) and other types of the low grade heat sources to power generations in order to utilize the waste heat as an energy source for power generation, desalination, cooling and other possible purposes which are more cost-effective than using the fossil fuel [11–14].

The ORC is a well-known plant, and it verified to be a valuable system to convert the sensible heat to mechanical power during the years. The KC is in competition with the ORC, specifically for the case of waste heat recovery [15]. Both the ORC and KC are potential alternatives for generating power from low temperature heat sources efficiently. Although the simple configuration of ORC can be accounted as its advantage due to its simplicity, reliability, and flexibility, the KC may have better performance from the second law perspective [16].

Many researches have been carried out for waste heat recovery by ORC. The working fluid of ORC has an important role in these cycles performance; therefore, some of the surveys focus on selection of best working fluid to gain the desired thermodynamic conditions [17–21]. Some other surveys have been performed on different configurations and comparing them with each other.

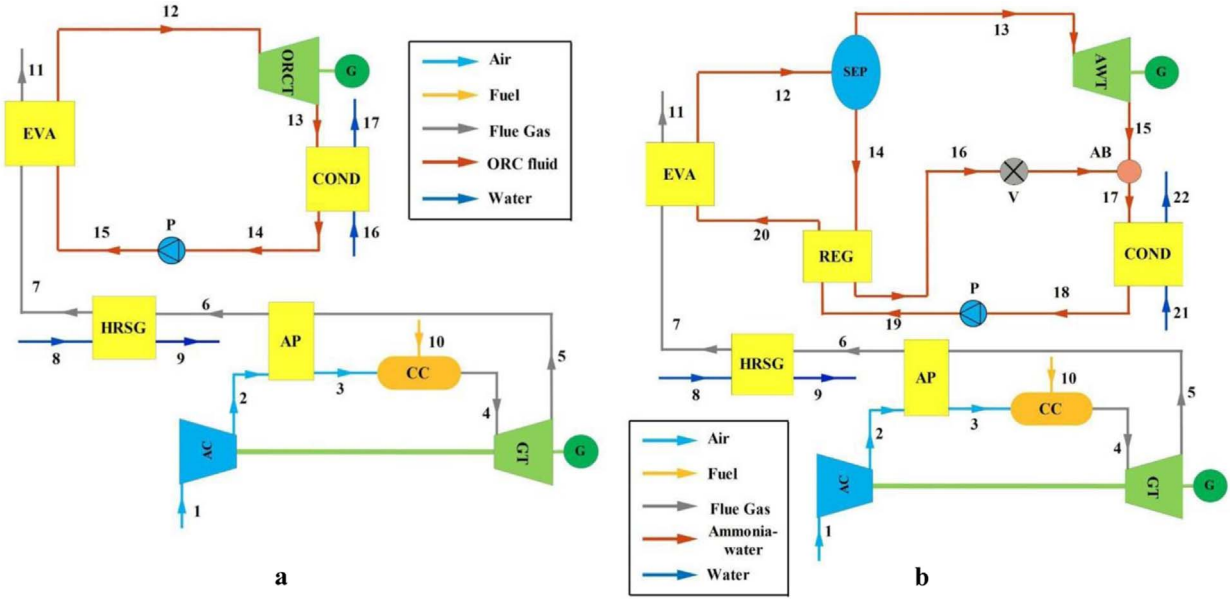

Fig. 1. Schematic diagram of the combined cysles. (a) CGAM/ORC (b) CGAM/KC (AC: Air compressor, AB: Absorber, AP: Air preheater, AWT: Ammonia water turbine, CC: Combustion chamber, COND: Condenser, Eva: Evaporator, GT: Gas turbine, G: Genarator, HRSG: Heat recovery steam generator, ORCT: Organic Rankine cycle turbine, P: Pump, REG: Regenerator, SEP: Separator, V: Valve).

There are various configurations of ORC i.e. the ORC with recuperator (RC), regenerative ORC (RG), organic flash cycle (OFC), trilateral (triangular) cycle (TLC) and some others. Each of mentioned configurations has some advantages and disadvantages and is suitable for a special purpose [22–27]. Mortaza Yari and S.M.S. Mahmoudi employed two ORC cycles to waste heat recovery from the GT-MHR cycle. They combined GT-MHR with these cycles and reported that both energy and exergy efficiencies, increase about 3%-points and exergy destruction rate decreases 5% in comparing to simple GT-MHR [13]. A. Sorourreddin et al. studied effect of different ORC configurations on waste heat recovery from GT-MHR system. They combined GT-MHR cycle with an ejector and an ORC unit (in different configurations) in order to waste heat recovery. They reported that in the best configuration at turbine inlet temperature of 850 °C, the energy efficiency is 15.86% higher than that of the simple GT-MHR cycle [28]. Shokati et al. published a comparative and parametric study of double flash and single flash ORCs with different working fluids. Their results showed that the highest values of energy efficiency and exergy efficiency among the mentioned cycles belong to single flash/ORC with steam [29].

The sample of the Kalina cycle was proposed in the early 1980s [30]. Afterwards, some other configurations of the Kalina cycle, such as KCS11, KCS 34, KCS34g and others were proposed [31,32]. There are a wide variety of researches in waste heat recovery by Kalina cycles. Zhang et al. outlined a review article to give comprehensive information about Kalina cycle, including description and introducing Kalina cycle, comparison of Kalina and Rankine cycle, first and second law analysis of Kalina cycle, different Kalina systems and different relationships to calculate thermodynamic properties of ammonia-water mixture [33]. Zare et al. employed a Kalina cycle in order to waste heat recovery of the GT-MHR cycle to produce additional power and they resulted that using Kalina cycle improves the second law efficiency of the GT-MHR cycle up to 4–10% [34]. Fallah et al. outlined an advanced exergy analysis of Kalina cycle, which applied for low temperature geothermal system. They examined the Kalina cycle from the viewpoint of advanced exergy which splits exergy destruction rate into endogenous, exogenous, avoidable and unavoidable parts [35]. Yari et al. studied Kalina cycle in comparison to TLC (trilateral Rankine cycle) and ORC systems. They considered a low-grade heat source with a temperature of 120 °C for all mentioned systems and reported that TLC can produce higher net output power than the ORC and Kalina (KCS11 (Kalina cycle system 11)) systems [36]. Rodriguez et al. compared a Kalina cycle (84% ammonia mass fraction) with an ORC unit (R-290 as working fluid) in order to use in low temperature enhanced geothermal system in Brazil. They reported that for the considered conditions, the Kalina cycle produces 18% more net power than the ORC [37]. A comparison between Kalina cycle and ORC for heat recovery from the diesel engine has performed by Bombarda et al. [15]. They concluded that the net output power is actually equal in value for Kalina and ORC systems, but the Kalina cycle requires a very high maximum pressure in order to obtain optimum thermodynamic performance.

To the best of the author's knowledge and by surveying the mentioned literature review, comparative thermodynamic analysis and optimization of ORC and Kalina cycle for waste heat recovery from the CGAM system are not performed. In order to cover the shortcomings existing in the literature, as a first step, thermodynamic models for combined CGAM/ORC and CGAM/KC systems are performed and influence of some significant decision variables such as the air compressor pressure ratio (r_p), the Kalina and ORC evaporator pressure (P_{EV}), the Kalina and ORC evaporator pinch point temperature difference (ΔT_{pp}), the ORC superheating degree (ΔT_{sup}) and the ammonia concentration (x_{12}) in Kalina cycle on the energy and exergy efficiencies, bottoming cycle net produced power and turbine size parameter are investigated.

2. System's description and assumptions

2.1. Combined CGAM/ORC

Fig. 1a indicates the schematic configuration of combined CGAM/ORC system. The CGAM cogeneration system consists of an air compressor (AC), a combustion chamber (CC), a high temperature gas turbine (GT), an air preheater (AP) and a heat recovery steam generator (HRSG) to produce steam as byproduct. Compressed air enters to combustion chamber and combustion products enter the GT at 1520 K to produce 30 MW net power. Expanded gas flows to AP to preheating the CC entering air and then provides the required heat source to produce 14 kg/s saturated steam at pressure of 20 bar [5]. HRSG exit gas flow offers required heat source for evaporator (EVA) to run an ORC unit. ORC working fluid pressurized in the pump and enters the evaporator in state 15. Evaporated working fluid flows to the ORC turbine and after producing power exists in the lower pressure level. Afterwards, it is cooled in the condenser and exists in saturated liquid condition.

2.2. Combined CGAM/KC

The schematic of the combined CGAM/KC is shown in Fig. 1b. Kalina cycle has several plant schemes in order to waste heat recovery as a bottoming cycle. In this study KCS11 is employed to waste heat recovery in CGAM cogeneration system. The HRSG exit gas flow provides the necessary driving energy of KCS11 system. KCS11 is designed especially to convert low-temperature heat into electricity. The evaporator exiting two-phase mixture is separated in the separator (state 12→13 and 12→14), the saturated vapor is expanded in the turbine to a lower pressure (state 13→15), and the saturated liquid flows into the regenerator to heat the pressurized mixture (state 14→16). The cooled regenerator exiting flow combines with the turbine exiting stream in the absorber, then mixed flow releases heat in the condenser and pressurizes by the pump.

2.3. Assumptions

Following assumption are made in this study for simplification:

- The system operates at steady state condition.
- Changes in the kinetic and potential exergy are negligible [38,39].
- The pressure losses in the ORC and KCS11 are not noticeable while in the CGAM cogeneration system some suggested values in literature [5] are considered for pressure losses.
- The cooling water enters the condenser at ambient condition [40,41].
- The molar analysis of air at the compressor inlet is: 77.48% N_2, 20.59% O_2, 0.03% CO_2 and 1.9% H_2O (g) [5].
- A complete combustion is considered in the combustion chamber and the low heating value of the methane (as fuel) is considered 802361 kJ/kmol [5].
- Heat loss in the combustion chamber is assumed to be 2% low heating value of fuel [5].
- The produced gas leaves the combustion chamber at 1520 K [5].
- The air compressor pressure ratio is $r_{p,AC} = 10$ [5].
- The turbine isentropic efficiency is 85% for all turbines in the alone CGAM and combined systems.
- The isentropic efficiency of AC and P are 85% and 75% respectively.
- Ambient temperature and pressure are 298.15 K and 1.013 bar, respectively.

3. Thermodynamic analyses

Solving coupled non-linear algebraic equations, resulted from systems modeling has been done by EES software [42]. Considering all components as a control volume, the consumed and produced powers associated with the compressor, pumps and turbines are calculated as follows [43]:

$$\eta_{C,\text{isen}} = \frac{\dot{W}_{C,isen}}{\dot{W}_C} \tag{1}$$

$$\eta_{T,isen} = \frac{\dot{W}_T}{\dot{W}_{T,isen}} \tag{2}$$

$$\eta_{P,isen} = \frac{\dot{W}_{P,isen}}{\dot{W}_P} \tag{3}$$

The thermal or energy efficiency for alone CGAM and combined cycles can be expressed as [44]:

$$\eta_{\text{thermal}} = \frac{output_{energy}}{\dot{n}_{fuel}\overline{LHV}_{fuel}} \tag{4}$$

here
$\overline{LHV}_{fuel}$ is the lower heating value of methane as fuel and $output_{energy}$ is the net produced power of the system as well as heat transferred in the HRSG.

The cost of components is directly related to their sizes [5]. The turbine size parameter is an indicator for size of turbine. For valuation of the actual turbine dimensioning, the turbine size parameter (*TSP*) can be defined as [45]:

Table 1
Relations used in energy and exergy analysis of the combined CGAM/ORC.

Components	Energy balance	Exergy balance
AC	$\eta_{is,AC} = \dot{W}_{is,AC}/\dot{W}_{AC}\dot{W}_{AC} = \dot{n}_1(h_2 - h_1)$	$\dot{E}_{D,AC} = \dot{W}_{AC} + \dot{n}_1\bar{e}_1 - \dot{n}_2\bar{e}_2\varepsilon_{AC} = (\dot{n}_2\bar{e}_2 - \dot{n}_1\bar{e}_1)/\dot{W}_{AC}$
AP	$\dot{n}_2h_2 + \dot{n}_5h_5 = \dot{n}_3h_3 + \dot{n}_6h_6$	$\dot{E}_{D,AP} = \dot{n}_2\bar{e}_2 + \dot{n}_5\bar{e}_5 - \dot{n}_3\bar{e}_3 - \dot{n}_6\bar{e}_6\varepsilon_{AP} = (\dot{n}_3\bar{e}_3 - \dot{n}_2\bar{e}_2)/(\dot{n}_5\bar{e}_5 - \dot{n}_6\bar{e}_6)$
CC	$\dot{n}_3h_3 + \dot{n}_{10}h_{10} = \dot{n}_4h_4$	$\dot{E}_{D,CC} = \dot{n}_3\bar{e}_3 + \dot{n}_{10}\bar{e}_{10} - \dot{n}_4\bar{e}_4\varepsilon_{CC} = \dot{n}_4\bar{e}_4/(\dot{n}_3\bar{e}_3 + \dot{n}_{10}\bar{e}_{10})$
GT	$\eta_{is,GT} = \dot{W}_{GT}/\dot{W}_{is,GT}\dot{W}_{GT} = \dot{n}_4(h_4 - h_5)$	$\dot{E}_{D,GT} = \dot{n}_4\bar{e}_4 - \dot{n}_5\bar{e}_5 - \dot{W}_{GT}\varepsilon_{GT} = \dot{W}_{GT}/(\dot{n}_4\bar{e}_4 - \dot{n}_5\bar{e}_5)$
HRSG	$\dot{n}_6h_6 + \dot{n}_8h_8 = \dot{n}_7h_7 + \dot{n}_9h_9$	$\dot{E}_{D,HRSG} = \dot{n}_6\bar{e}_6 + \dot{n}_8\bar{e}_8 - \dot{n}_7\bar{e}_7 - \dot{n}_9\bar{e}_9\varepsilon_{HRSG} = (\dot{n}_9\bar{e}_9 - \dot{n}_8\bar{e}_8)/(\dot{n}_6\bar{e}_6 - \dot{n}_7\bar{e}_7)$
EVA	$\dot{n}_7h_7 + \dot{n}_{15}h_{15} = \dot{n}_{11}h_{11} + \dot{n}_{12}h_{12}$	$\dot{E}_{D,EVA} = \dot{n}_7\bar{e}_7 + \dot{n}_{15}\bar{e}_{15} - \dot{n}_{11}\bar{e}_{11} - \dot{n}_{12}\bar{e}_{12}\varepsilon_{EVA} = (\dot{n}_{12}\bar{e}_{12} - \dot{n}_{15}\bar{e}_{15})/(\dot{n}_7\bar{e}_7 - \dot{n}_{11}\bar{e}_{11})$
ORCT	$\eta_{is,ORCT} = \dot{W}_{ORCT}/\dot{W}_{is,ORCT}\dot{W}_{ORCT} = \dot{n}_{12}(h_{12} - h_{13})$	$\dot{E}_{D,ORCT} = \dot{n}_{12}\bar{e}_{12} - \dot{n}_{13}\bar{e}_{13} - \dot{W}_{ORCT}\varepsilon_{ORCT} = \dot{W}_{ORCT}/(\dot{n}_{12}\bar{e}_{12} - \dot{n}_{13}\bar{e}_{13})$
COND	$\dot{n}_{13}h_{13} + \dot{n}_{16}h_{16} = \dot{n}_{14}h_{14} + \dot{n}_{17}h_{17}$	$\dot{E}_{D,COND} = \dot{n}_{13}\bar{e}_{13} + \dot{n}_{16}\bar{e}_{16} - \dot{n}_{14}\bar{e}_{14} - \dot{n}_{17}\bar{e}_{17}\varepsilon_{COND} = (\dot{n}_{17}\bar{e}_{17} - \dot{n}_{16}\bar{e}_{16})/(\dot{n}_{13}\bar{e}_{13} - \dot{n}_{14}\bar{e}_{14})$
p	$\eta_{is,P} = \dot{W}_{is,P}/\dot{W}_P\dot{W}_P = \dot{n}_{14}(h_{15} - h_{14})$	$\dot{E}_{D,P} = \dot{W}_P + \dot{n}_{14}\bar{e}_{14} - \dot{n}_{15}\bar{e}_{15}\varepsilon_P = (\dot{n}_{15}\bar{e}_{15} - \dot{n}_{14}\bar{e}_{14})/\dot{W}_P$

$$TSP = \frac{\sqrt[2]{\dot{n}_{wf}\,\overline{v}_{out,is}}}{\sqrt[4]{\overline{h}_{in} - \overline{h}_{out,is}}} \tag{5}$$

where $\dot{n}_{wf}$ is working fluid molar flow rate, $\overline{v}_{out,is}$ is specific volume of the turbine outlet at isentropic condition, $\overline{h}_{in}$ is turbine inlet specific enthalpy and $\overline{h}_{out,is}$ is turbine outlet specific enthalpy at isentropic condition.

Eq. (6) presents the exergy balance for an energy system [46]:

$$\sum_{in} \dot{E}_i = \sum_{out} \dot{E}_j + \dot{E}_D + \dot{E}_L \tag{6}$$

where, $\sum_{in} \dot{E}_i$ and $\sum_{out} \dot{E}_j$ are inlet and outlet exergy rates of the system. $\dot{E}_D$ and $\dot{E}_L$ represent the rate of exergy destruction and exergy loss, respectively.

Ignoring the kinetic and potential exergy changes, the specific exergy of a stream is the sum of the specific physical exergy ($e_{ph,i}$) and specific chemical exergy ($e_{ch,i}$):

$$e_i = e_{ph,i} + e_{ch,i} \tag{7}$$

Accordingly, the exergy rate of each stream will be:

$$\dot{E}_i = \dot{n}_i e_i \tag{8}$$

The specific physical exergy of a stream depends on its temperature and pressure as well as the ambient condition [47–49]:

$$e_i^{ph} = h_i - h_0 - T_0(s_i - s_0) \tag{9}$$

here, *0* demonstrates the restricted dead state condition.

For a mixture of ideal gases the specific chemical exergy can be expressed as [46]:

$$e_{mixture}^{ch} = \sum_i n_i e_{0,i}^{ch} + \overline{R} T_0 \sum n_i \ln x_i \tag{10}$$

here, $e_{0,i}^{ch}$ and x_i stand for the standard chemical exergy and molar fraction of the ith mixture component.

To define the exergy efficiency and exergy destruction of a component, it is essential to specify the fuel and product definition for each component which is defined in exergy terms. Exergy efficiency indicates the percentage of provided fuel exergy to a system that is found in the product exergy. Exergy destruction and exergy efficiency of each component are as follows [5,13,44]:

$$\dot{E}_D = \dot{E}_F - \dot{E}_P \tag{11}$$

$$\varepsilon = \frac{\dot{E}_P}{\dot{E}_F} \tag{12}$$

The total exergy efficiency for alone CGAM and combined cycles is defined as the ratio of net produced power plus exergy of produced steam to the input exergy, as follows [5]:

Table 2
Relations used in energy and exergy analysis of the combined CGAM/KC.

Components	Energy balance	Exergy balance
AC	$\eta_{is,AC} = \dot{W}_{is,AC}/\dot{W}_{AC}\dot{W}_{AC} = \dot{n}_1(h_2 - h_1)$	$\dot{E}_{D,AC} = \dot{W}_{AC} + \dot{n}_1\bar{e}_1 - \dot{n}_2\bar{e}_2\varepsilon_{AC} = (\dot{n}_2\bar{e}_2 - \dot{n}_1\bar{e}_1)/\dot{W}_{AC}$
AP	$\dot{n}_2h_2 + \dot{n}_5h_5 = \dot{n}_3h_3 + \dot{n}_6h_6$	$\dot{E}_{D,AP} = \dot{n}_2\bar{e}_2 + \dot{n}_5\bar{e}_5 - \dot{n}_3\bar{e}_3 - \dot{n}_6\bar{e}_6\varepsilon_{AP} = (\dot{n}_3\bar{e}_3 - \dot{n}_2\bar{e}_2)/(\dot{n}_5\bar{e}_5 - \dot{n}_6\bar{e}_6)$
CC	$\dot{n}_3h_3 + \dot{n}_{10}h_{10} = \dot{n}_4h_4$	$\dot{E}_{D,CC} = \dot{n}_3\bar{e}_3 + \dot{n}_{10}\bar{e}_{10} - \dot{n}_4\bar{e}_4\varepsilon_{CC} = \dot{n}_4\bar{e}_4/(\dot{n}_3\bar{e}_3 + \dot{n}_{10}\bar{e}_{10})$
GT	$\eta_{is,GT} = \dot{W}_{GT}/\dot{W}_{is,GT}\dot{W}_{GT} = \dot{n}_4(h_4 - h_5)$	$\dot{E}_{D,GT} = \dot{n}_4\bar{e}_4 - \dot{n}_5\bar{e}_5 - \dot{W}_{GT}\varepsilon_{GT} = \dot{W}_{GT}/(\dot{n}_4\bar{e}_4 - \dot{n}_5\bar{e}_5)$
HRSG	$\dot{n}_6h_6 + \dot{n}_8h_8 = \dot{n}_7h_7 + \dot{n}_9h_9$	$\dot{E}_{D,HRSG} = \dot{n}_6\bar{e}_6 + \dot{n}_8\bar{e}_8 - \dot{n}_7\bar{e}_7 - \dot{n}_9\bar{e}_9\varepsilon_{HRSG} = (\dot{n}_9\bar{e}_9 - \dot{n}_8\bar{e}_8)/(\dot{n}_6\bar{e}_6 - \dot{n}_7\bar{e}_7)$
EVA	$\dot{n}_7h_7 + \dot{n}_{20}h_{20} = \dot{n}_{11}h_{11} + \dot{n}_{12}h_{12}$	$\dot{E}_{D,EVA} = \dot{n}_7\bar{e}_7 + \dot{n}_{20}\bar{e}_{20} - \dot{n}_{11}\bar{e}_{11} - \dot{n}_{12}\bar{e}_{12}\varepsilon_{EVA} = (\dot{n}_{12}\bar{e}_{12} - \dot{n}_{20}\bar{e}_{20})/(\dot{n}_7\bar{e}_7 - \dot{n}_{11}\bar{e}_{11})$
AWT	$\eta_{is,AWT} = \dot{W}_{AWT}/\dot{W}_{is,AWT}\dot{W}_{AWT} = \dot{n}_{13}(h_{13} - h_{15})$	$\dot{E}_{D,AWT} = \dot{n}_{13}\bar{e}_{13} - \dot{n}_{15}\bar{e}_{15} - \dot{W}_{AWT}\varepsilon_{AWT} = \dot{W}_{AWT}/(\dot{n}_{13}\bar{e}_{13} - \dot{n}_{15}\bar{e}_{15})$
COND	$\dot{n}_{17}h_{17} + \dot{n}_{21}h_{21} = \dot{n}_{18}h_{18} + \dot{n}_{22}h_{22}$	$\dot{E}_{D,COND} = \dot{n}_{17}\bar{e}_{17} + \dot{n}_{21}\bar{e}_{21} - \dot{n}_{18}\bar{e}_{18} - \dot{n}_{22}\bar{e}_{22}\varepsilon_{COND} = (\dot{n}_{22}\bar{e}_{22} - \dot{n}_{21}\bar{e}_{21})/(\dot{n}_{17}\bar{e}_{17} - \dot{n}_{18}\bar{e}_{18})$
p	$\eta_{is,P} = \dot{W}_{is,P}/\dot{W}_P\dot{W}_P = \dot{n}_{18}(h_{19} - h_{18})$	$\dot{E}_{D,P} = \dot{W}_P + \dot{n}_{18}\bar{e}_{18} - \dot{n}_{19}\bar{e}_{19}\varepsilon_P = (\dot{n}_{19}\bar{e}_{19} - \dot{n}_{18}\bar{e}_{18})/\dot{W}_P$
REGEN	$\dot{n}_{19}h_{19} + \dot{n}_{14}h_{14} = \dot{n}_{20}\bar{e}_{20} + \dot{n}_{16}\bar{e}_{16}$	$\dot{E}_{D,REGEN} = \dot{n}_{19}\bar{e}_{19} + \dot{n}_{14}\bar{e}_{14} - \dot{n}_{20}\bar{e}_{20} - \dot{n}_{16}\bar{e}_{16}$ $\varepsilon_{REGEN} = (\dot{n}_{20}\bar{e}_{20} - \dot{n}_{19}\bar{e}_9)/(\dot{n}_{14}\bar{e}_{14} - \dot{n}_{16}\bar{e}_{16})$

Table 3
Comparison between the Bejan et al.'s results and present work for Bejan et al.'s configuration.

System	Performance parameters	Bejan [5]	Present study	Error (%)
CGAM	Fuel-air ratio	0.0321	0.033	2.8
	Energy efficiency [%]	–	88.65	–
	Exergy efficiency [%]	50.3	49.9	0.8
KC	Performance parameters	Ogriseck [51]	Present study	Error (%)
	Net output power [kW]	2194.8	2186.1	0.4
	Electrical efficiency [%]	16.8	16.68	0.7
ORC	Performance parameters	Yari [52]	Present study	Error (%)
	Net output specific work [kJ/kg]	48.57	49.03	0.9
	Energy efficiency [%]	12.6	12.63	0.2
	Exergy Effiiency [%]	46.8	46.85	0.1

$$\varepsilon_{total} = \frac{\dot{W}_{net} + \dot{E}_{29} - \dot{E}_9}{\dot{E}_{in}} \tag{13}$$

where $\dot{W}_{net}$ is the total produced power in turbines minus consumed power by the compressor and pump.

The entering exergy to the system can be expressed as:

$$\dot{E}_{in} = \dot{E}_1 + \dot{E}_{10} \tag{14}$$

In Eq. (12), the term of $\dot{E}_{29} - \dot{E}_9$ refers to exergy of the produced steam in HRSG as a byproduct.

The relations used in energy and exergy analyses of the combined systems are outlined in Tables 1 and 2.

4. Model validation

In order to validate the developed simulation model of the proposed combined systems, the reported data in the literature [5,50–52] is used. The validation performed for the CGAM cogeneration system, KC and ORC. Table 3 indicates a comparison between the results of the present model for the CGAM, KC and ORC systems and the results reported by literature [5,51,52]. Results of Table 3 are based on the same values of input parameters with those studied in literatures. In presented comparison, for the case of ORC, the considered working fluid is *n*-Pantane. Referring to Table 3, maximum error between the obtained results and those reported in literatures is 2.8% for fuel-air ratio of CGAM system while other compared parameters have less than 1% difference. Also, Fig. 2 represents a comparison between the results of the present model for the Kalina cycle and the results reported by Hettiarachchi et al. [50] for energy efficiency. Referring to Table 3 and Fig. 2, there are good agreements between the obtained results in the present model and those reported in the literature. Therefore, it can be concluded that the numerical calculation of the systems thermodynamic modeling is reliable.

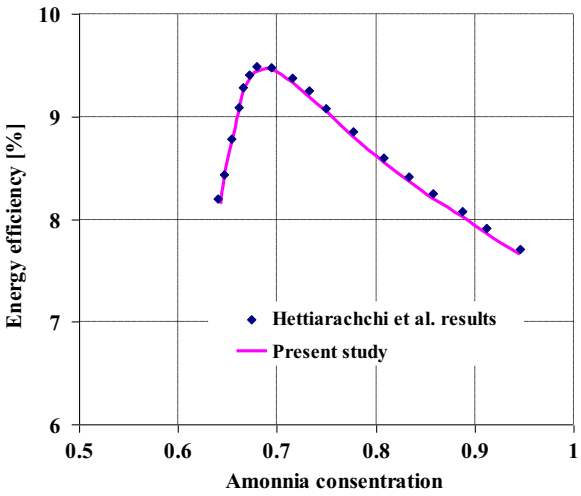

Fig. 2. Comparison between Hettiarachchi results [50] and present study for KCS11 energy efficiency.

Table 4
Calculated thermodynamic properties and mass flow rates for combined CGAM/ORC.

Stream	Fluid	Pressure (bar)	Temperature (K)	Molar flow rate (kmol/s)
1	N_2, O_2, CO_2, H_2O	1.013	298.15	2.46, 0.654, 0.001, 0.06
2	N_2, O_2, CO_2, H_2O	10.13	610.8	2.46, 0.654, 0.001, 0.06
3	N_2, O_2, CO_2, H_2O	9.624	850	2.46, 0.654, 0.001, 0.06
4	N_2, O_2, CO_2, H_2O	9.142	1520	2.46, 0.449, 0.1, 0.265
5	N_2, O_2, CO_2, H_2O	1.099	1011	2.46, 0.449, 0.1, 0.265
6	N_2, O_2, CO_2, H_2O	1.066	793.1	2.46, 0.449, 0.1, 0.265
7	N_2, O_2, CO_2, H_2O	1.013	429	2.46, 0.449, 0.1, 0.265
8	H_2O	20	298.15	0.777
9	H_2O	20	485.6	0.777
10	CH_4	12	298.15	0.1024
11	N_2, O_2, CO_2, H_2O	1.013	327.4	2.46, 0.449, 0.1, 0.265
12	R245fa	10	367.8	0.3098
13	R245fa	1.478	320	0.3098
14	R245fa	1.478	298.15	0.3098
15	R245fa	10	298.6	0.3098
16	H_2O	1.013	298.15	11.63
17	H_2O	1.013	308.15	11.63

Table 5
Calculated thermodynamic properties and mass flow rates for combined CGAM/KC.

Stream	Fluid	Pressure (bar)	Temperature (K)	Molar flow rate (kmol/s)	Ammonia concentration (kg NH3/kg solution)
1	N_2, O_2, CO_2, H_2O	1.013	298.15	2.46, 0.654, 0.001, 0.06	–
2	N_2, O_2, CO_2, H_2O	10.13	610.8	2.46, 0.654, 0.001, 0.06	–
3	N_2, O_2, CO_2, H_2O	9.624	850	2.46, 0.654, 0.001, 0.06	–
4	N_2, O_2, CO_2, H_2O	9.142	1520	2.46, 0.449, 0.1, 0.265	–
5	N_2, O_2, CO_2, H_2O	1.099	1011	2.46, 0.449, 0.1, 0.265	–
6	N_2, O_2, CO_2, H_2O	1.066	793.1	2.46, 0.449, 0.1, 0.265	–
7	N_2, O_2, CO_2, H_2O	1.013	429	2.46, 0.449, 0.1, 0.265	–
8	H_2O	20	298.15	0.777	–
9	H_2O	20	485.6	0.777	–
10	CH_4	12	298.15	0.1024	–
11	N_2, O_2, CO_2, H_2O	1.013	327.4	2.46, 0.449, 0.1, 0.265	–
12	NH_3H_2O	50	415	5.848	0.9
13	NH_3H_2O	50	415	5.121	0.9543
14	NH_3H_2O	50	415	0.7272	0.5173
15	NH_3H_2O	10.61	341.5	5.121	0.9543
16	NH_3H_2O	50	336.1	0.7272	0.5173
17	NH_3H_2O	10.61	340	5.848	0.9
18	NH_3H_2O	10.61	303.15	5.848	0.9
19	NH_3H_2O	50	304.3	5.848	0.9
20	NH_3H_2O	50	314.4	5.848	0.9
21	H_2O	1.013	298.15	11.63	–
22	H_2O	1.013	308.15	11.63	–

5. Results

5.1. Parametric study

The values of thermodynamic properties in each point of combined systems in particular operating conditions are represented in Tables 4 and 5 for CGAM/ORC and CGAM/KC, respectively.

A parametric study is performed to investigate the effects of some important parameters on the performance of combined cycles. Based on the literatures [37,53], the influences of some significant decision variables on the CGAM/ORC performance, such as the air compressor pressure ratio (r_p), the evaporator pressure (P_{EV}), the pinch point temperature difference (ΔT_{pp}) and the superheating degree (ΔT_{sup}) have been investigated. In the parametric study of CGAM/KC, the air compressor pressure ratio (r_p), the evaporator pressure (P_{EV}), the pinch point temperature difference (ΔT_{pp}) and the ammonia concentration (x_{12}) are considered as decision variables.

5.1.1. Effect of main cycle parameter (CGAM cogeneration system)

Fig. 3a shows the effect of r_p on the first and second law efficiencies, ORC net output power and molar flow rate of fuel in the CGAM/ORC system. Referring to Fig. 3a, the change in the r_p maximizes the energy and exergy efficiencies while the ORC net output power and the molar flow rate of fuel trend reverse with efficiencies. In spite of minimizing the ORC produced power, due to

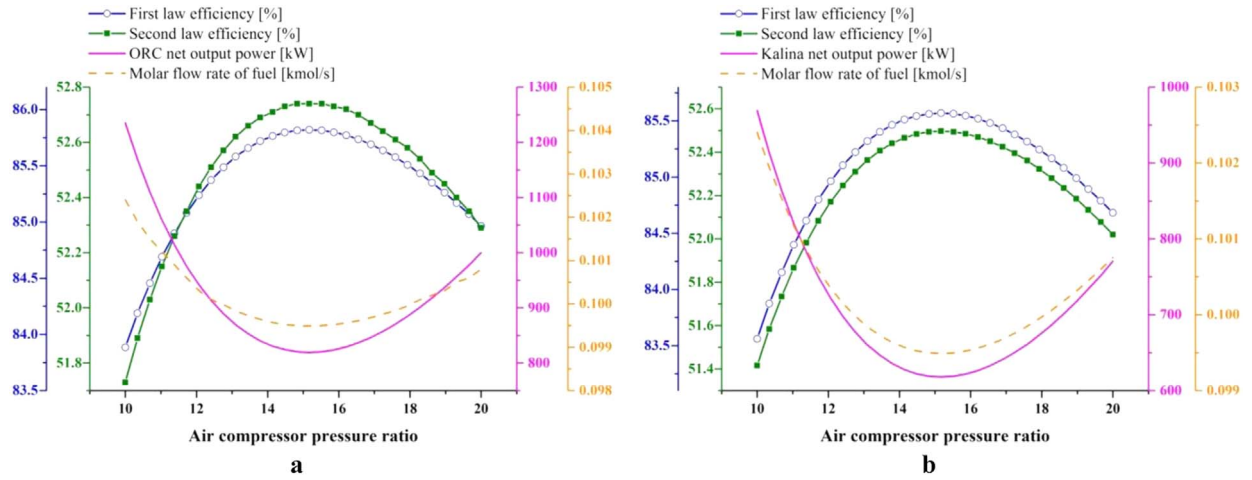

Fig. 3. Effect of r_p on first and second law efficiencies, net output power and molar flow rate of fuel. (a) CGAM/ORC (b) CGAM/KC.

minimizing the molar flow rate of consumed fuel, the energy and exergy efficiencies will be maximized (see Fig. 3a).

Effects of r_p on the first and second law efficiencies, the Kalina net output power and the molar flow rate of fuel in CGAM/KC system are shown in Fig. 3b. Referring to Fig. 3b, the behavior of the mentioned parameters in the CGAM/KC by varying the air compressor pressure ratio are the same as CGAM/ORC system, but the values of these parameters differ. For example, maximum exergy efficiency of CGAM/ORC is 52.74%, while it is 52.49% for the CGAM/KC. The behavior of parameters in Fig. 3b can justified same as Fig. 3a.

Fig. 4a represents variation of the ORC evaporator inlet gas temperature (T_7), the ORC evaporator outlet gas temperature (T_{11}), ORC working fluid molar flow rate and ORC turbine size parameter (TSP) by change in the air compressor pressure ratio. Also, Fig. 4b indicates variation of the same parameters for the CGAM/KC system. As can be seen, in pressure ratio of about 15, the temperature difference between the inlet and outlet hot gases to the ORC evaporator is the lowest and as a result the enthalpy difference between state 7 and 11, which is the energy source of ORC, is low too. On the other hand, the working fluid molar flow rate has a minimum value in a particular r_p. Both of these parameters have straight effect on the net output power of ORC, which results in minimization of produced power by the ORC (see Fig. 3a). Furthermore, working fluid molar flow rate has a direct effect on TSP (see Eq. (5)). Therefore, TSP changes same as working fluid molar flow rate by varying r_p. Fig. 4b depicts that the CGAM/KC parameters behave same as the CGAM/ORC system. By comparison of Fig. 4a and b, it can be concluded that the Kalina evaporator outlet gas temperature is higher than that of the ORC combined system. This means that the utilized waste energy by CGAM/KC system is less than the CGAM/ORC system.

5.1.2. *Effect of buttoming cycles parameters (KC and ORC)*

The Effect of the pinch point temperature difference (ΔT_{pp}) on the first and second law efficiencies, the ORC net output power,

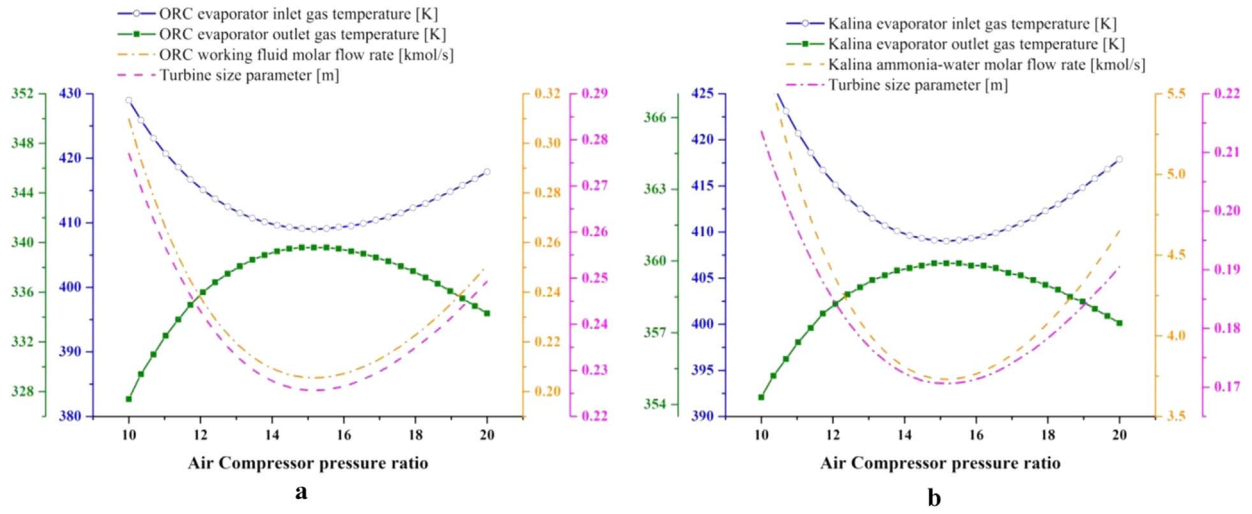

Fig. 4. Variation of the evaporator inlet and outlet gas temperature (T_7, T_{11}), turbine size parameter and working fluid molar flow rate by varying the r_p. (a) CGAM/ORC (b) CGAM/KC.

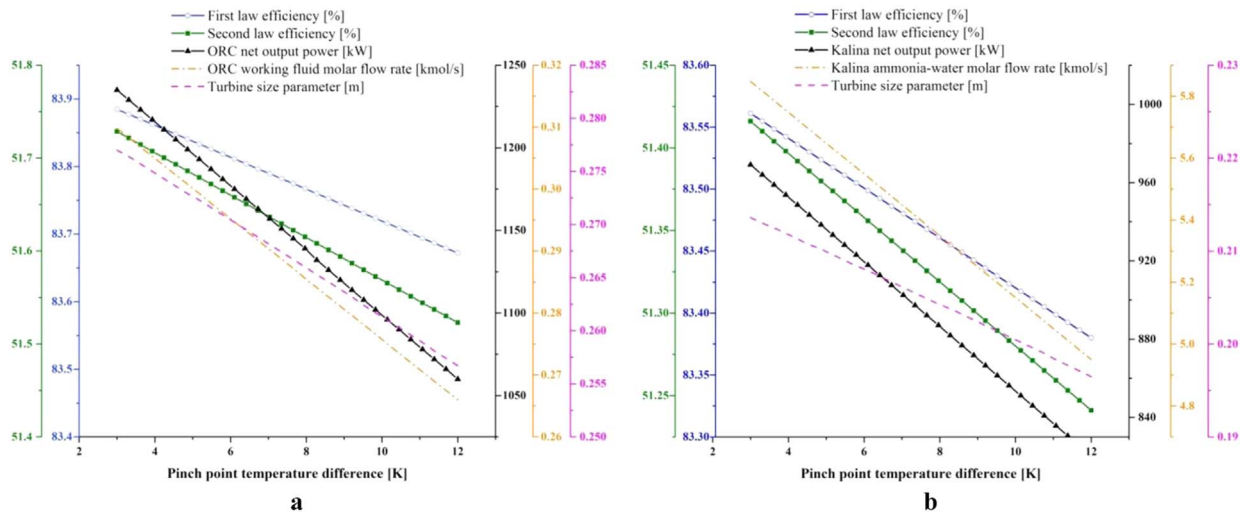

Fig. 5. Effect of the pinch point temperature difference (ΔT_{pp}) on the first and second law efficiencies, net output power, turbine size parameter and working fluid molar flow rate. (a) CGAM/ORC (b) CGAM/KC.

the ORC working fluid molar flow rate and the turbine size parameter (TSP) is presented in Fig. 5a. The pinch point temperature difference only affects the bottoming cycle (ORC) performance and increase in this parameter leads to decrease of attainable energy from the CGAM. Because all of the base cycle (CGAM) specifications such as inlet and outlet exergy remain constant by varying the pinch point temperature difference, energy and exergy efficiencies have the same trend with the ORC net output power that leads to reduction of these efficiencies by increasing the pinch point temperature difference. Referring to Fig. 5a, TSP trends same as the working fluid molar flow rate. Changing same parameters for the CGAM/KC by varying the pinch point temperature difference (ΔT_{pp}) is presented in Fig. 5b, which shows the same trends with CGAM/ORC system parameters. Increasing ΔT_{pp} from 3 to 12 leads to decrease in ORC net power from 1234.97 to 1060 kW, and Kalina net power from 969 to 820.3 kW, which means 14.17% generated power reduction for the ORC and 15.35% of the Kalina produced power. On the other hand, it is valuable mentioning that the Kalina working fluid molar flow rate is about 18 times more than that of ORC.

Fig. 6a reveals variation of the first and second law efficiencies, the ORC net output power, the ORC working fluid molar flow rate, the ORC turbine inlet enthalpy and the turbine size parameter by change in the ORC evaporator pressure (P_{ev}). The effect of the Kalina evaporator pressure on the first and second law efficiencies, the Kalina net output power and the ammonia-water molar flow rate is presented in Fig. 6b. The performance of the base cycle (CGAM) is not affected by the change in this variable. Therefore, only the bottoming cycle performance changes by varying P_{ev}. Consequently, as it can be seen in Fig. 6a, the energy and exergy efficiencies behave same as the net output power of ORC. By increasing the evaporator pressure from 7 to 18 bar, the generated power via ORC increases first then decreases. Increasing the evaporator pressure has two conflicting effects on the ORC produced power: the first one is increasing the turbine inlet enthalpy which leads to more power generation by the ORC and the second one is

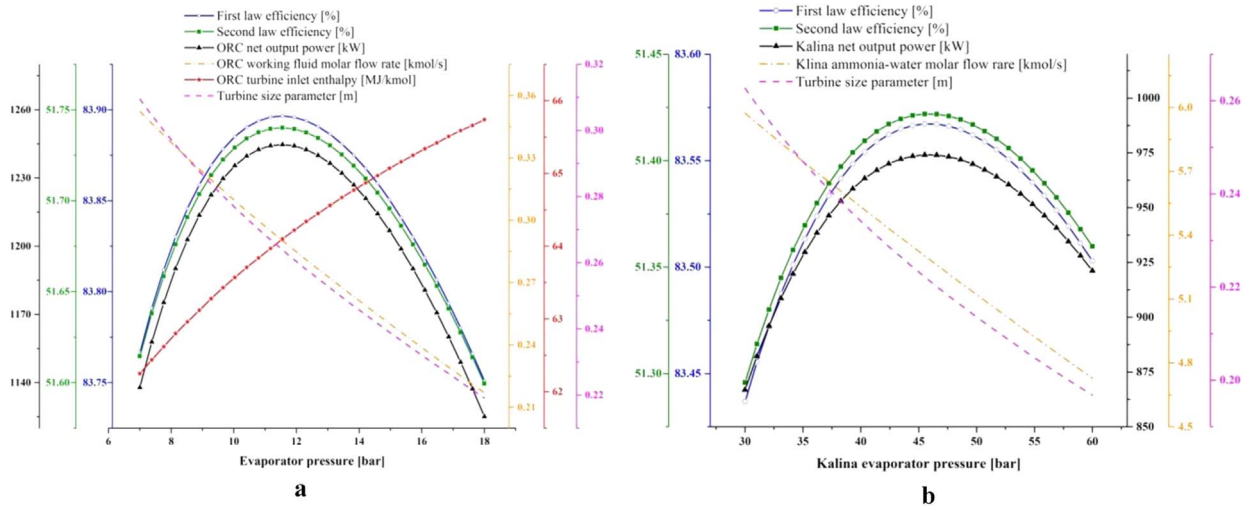

Fig. 6. Effect of evaporator pressure (P_{ev}) on the first and second law efficiencies, net output power, working fluid molar flow rate, turbine size parameter and ORC turbine inlet enthalpy. (a) CGAM/ORC (b) CGAM/KC.

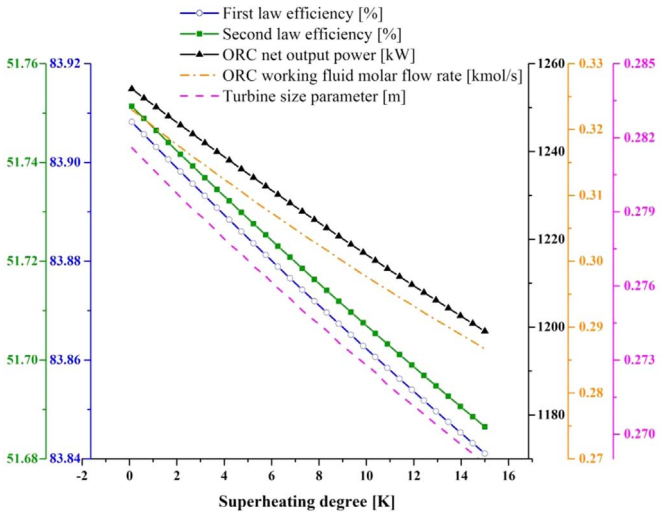

Fig. 7. Effect of superheating degree (ΔT_{sup}) on the first and second law efficiencies, ORC net output power and ORC working fluid molar flow rate.

decreasing the molar flow rate of ORC working fluid which reduced the produced power. It is observed that for lower values of P_{ev}, the dominant effect is the first one which leads to increase in the ORC power generation and in higher values of P_{ev} the second effect is the main one that results in decreasing the ORC net output power. The consequence of these effects is maximizing the ORC net output power as it is illustrated in Fig. 6a. Increasing the evaporator pressure, leads to decrease in the working fluid molar flow rate and increase in the turbine inlet enthalpy, which both of these variations cause to decline the TSP. Trends of CGAM/KC performance by varying the evaporator pressure, which is illustrated in Fig. 6b is the same as CGAM/KC system. The most significant difference between these two systems is their optimum pressure. Referring to Fig. 6a and b, the optimum pressure for the CGAM/ORC is about 11 bar, while the optimum pressure for the CGAM/KC system is about 46 bar. Furthermore, by a close look to Figs. 3–6, it can be concluded that the Kalina turbine size parameter is less than that of the ORC, which can be an advantage of the Kalina cycle in comparison to the ORC.

The effect of the superheating degree (ΔT_{sup}) on the first and second law efficiencies, the ORC net output power, the ORC working fluid molar flow rate and the turbine size parameter is indicated in Fig. 7. Like the effect of the pinch point temperature difference, the superheating degree doesn't have any effect on the base cycle. Therefore, the first and second law efficiencies only affected by the ORC net output power. With increasing the superheating degree, the turbine inlet enthalpy (state 12 for ORC in Fig. 1a) increase which leads to growing of the turbine power generation and increasing the ORC net output power. On the other hand, an increase in the superheating degree decreases the ORC working fluid molar flow rate that has a negative effect on the ORC net output power. The simultaneous effect of these two contrary effects is decreasing the ORC net output power, which means working fluid molar flow rate effect is the prevailing one. Increasing the superheating degree leads to decreasing the working fluid molar flow rate and turbine inlet enthalpy which cause reduction of the turbine size parameter.

Fig. 8 shows change in the first and second law efficiencies, the Kalina net output power, the separator inlet quality and the

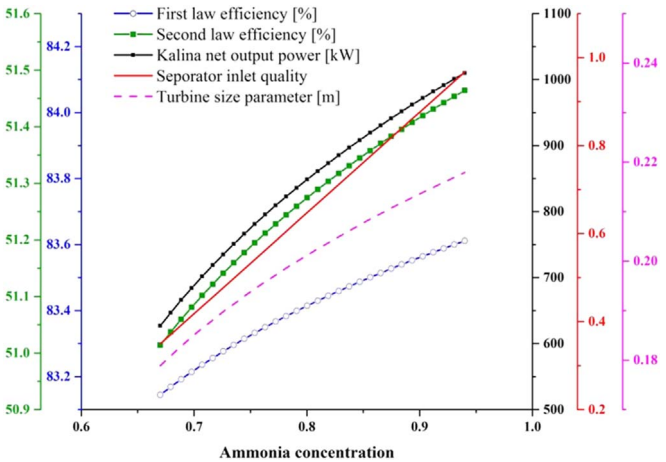

Fig. 8. Effect of ammonia density (x_{12}) on the first and second law efficiencies, Kalina net output power, Kalina working fluid molar flow rate and turbine size parameter.

Table 6
The results of performance optimization for Combined CGAM/ORC and CGAM/KC systems.

Decision variable/performance parameters	Combined CGAM/ORC	Combined CGAM/KC
Compressor pressure ratio	15.13	15.19
Minimum temperature difference in evaporator [°C]	3	3
Degree of superheat [°C]	0	–
Ammonia mass fraction [%]	–	94
Exergy efficiency [%]	52.77	52.58
$\dot{W}_{net,ORC/Kalina}$ [kW]	844.3	688.8
$P_{High,ORC/Kalina}$ [bar]	10.816	38.17
Turbine outlet quality	superheat	0.94
TSP	0.2385	0.2042

turbine size parameter by varying the ammonia concentration (x) in the separator inlet (state 12). Ammonia-water quality in the separator inlet which is state 12 in Fig. 1b increases by increasing the ammonia concentration as it can be seen in Fig. 8. This leads to increase in the working fluid molar flow rate, which flows to the Kalina turbine and causes growing the Kalina net output power. Since the ammonia concentration only affects the Kalina cycle performance, the energy and exergy efficiencies vary same as the net Kalina produced power. Kalina turbine inlet molar flow rate grows by increasing the ammonia concentration, which leads to TSP increasing.

5.2. Optimization

In order to optimization purposes, exergy efficiency of the combined system is considered as objective function. Decision variables associated with optimization are the mentioned parameters in parametric study section. Using direct search method by the EES software, the performance of the combined systems is optimized from the viewpoint of exergy efficiency. Direct search methods are the best known as unconstrained optimization techniques that do not explicitly use derivatives [54].

For the combined CGAM/ORC:
Maximize exergy efficiency ($r_p, P_{EV}, \Delta T_{pp}, \Delta T_{sup}$)
For the combined CGAM/KC:
Maximize exergy efficiency ($r_p, P_{EV}, \Delta T_{pp}, x_{19}$)

It is worth mentioning that, in order to CGAM/KC exergy efficiency optimization, the ammonia-water quality at the turbine exit limits the upper bound of x_{19} in such a way that the ammonia-water quality should be higher than 0.9 [55].

Results of optimization for both combined CGAM/ORC and CGAM/KC are outlined in Table 6. Referring to Table 6, under the optimized condition, the produced net power of the ORC is 22.57% more than that of the Kalina cycle. Table 6 also indicates that the exergy efficiency of combined CGAM/ORC is slightly higher than that of the CGAM/KC (under the optimized condition, the CGAM/ORC has the exergy efficiency of 52.77% while the CGAM/KC has the exergy efficiency of 52.58%) while the high pressure of combined CGAM/KC (38.17 bar) is much higher than that of CGAM/ORC (10.816 bar) and this can be an advantage of combined CGAM/ORC system. In addition, the state of working fluid in the turbine exit is two-phase flow for the Kalina while it is superheated vapor for the ORC. When turbine exit flow is superheated vapor, it has some advantages like avoiding droplet erosion, allowing reliable operation and fast start-up. Based on the optimized results, the CGAM/ORC has the TSP of 0.2385 while the CGAM/KC has the TSP of 0.2042. Therefore, by comparison of turbine size parameter for Kalina cycle and ORC, it is observed that the Kalina cycle is better than the ORC, which is the only advantage of Kalina cycle. By comparison of these cycles and with attention to the simplicity of ORC, it can be valuable mentioning that in order to waste heat recovery from CGAM cogeneration system, ORC is a more promising system than Kalina.

6. Conclusion

Thermodynamic modeling and optimization are performed for two combined cogeneration systems: CGAM/ORC and CGAM/KC which utilize CGAM waste heat for power generation. The main conclusions that can be obtained from the present work are listed as follows:

- Varying the air compressor pressure ratio optimizes the first and second law efficiencies in particular pressure ratio, whereas the bottoming cycle net output power and TSP are minimized.
- An increase in the pinch point temperature difference decreases the energy and exergy efficiencies, bottoming cycle power generation and TSP.
- First and second law efficiencies and bottoming cycle net output power are optimized with evaporator pressure. But turbine size parameter decreases with increasing the evaporator pressure.
- Increasing the superheating degree has a negative effect on the CGAM/ORC performance. Increasing superheating degree from 0

to 15 °C decreases the ORC net output power about 60 kW.

- Growing the ammonia concentration in the Kalina cycle increases the energy and exergy efficiencies, power generation and TSP.
- For all operating conditions, energy and exergy efficiencies of the CGAM/ORC system are more than those of the CGAM/KC which shows that the ORC is a promising option for waste heat recovery from CGAM.
- The optimum pressure value for the ORC is much lower than that of the Kalina which leads to lower cost levels for materials and sealing of ORC.
- Another advantage of the ORC is that the ORC turbine outlet is superheated vapor while the Kalina cycle turbine outlet is two-phase flow.
- Turbine size parameter for the Kalina cycle is lower than that of the ORC (TSP for the Kalina is 17% less than that of the ORC at optimum condition) which is the positive aspect of Kalina in comparison to the ORC.

References

[1] EIA, US. Energy Information Administration (2010). International Energy Outlook 2010—Highlights. Report DOE/EIA-0484, 2010.
[2] Antonio Valero, et al., CGAM problem: definition and conventional solution, Energy 19(3) (1994) 279–286.
[3] Christos A. Frangopoulos, Application of the thermoeconomic functional approach to the CGAM problem, Energy 19(3) (1994) 323–342.
[4] Michael R. von Spakovsky, Application of engineering functional analysis to the analysis and optimization of the CGAM problem, Energy 19(3) (1994) 343–364.
[5] Adrian Bejan, George Tsatsaronis, Thermal design and optimization, John Wiley & Sons, 1996.
[6] Antonio Valero, et al., CGAM problem: definition and conventional solution, Energy 19(3) (1994) 279–286.
[7] George Tsatsaronis, Javier Pisa, Exergoeconomic evaluation and optimization of energy systems—application to the CGAM problem, Energy 19(3) (1994) 287–321.
[8] A. Valero, et al., Application of the exergetic cost theory to the CGAM problem, Energy 19(3) (1994) 365–381.
[9] Eurostat, Ten00115. Electricity prices for household consumers. Tech. rep., European Union, 2013.
[10] U.S. Energy Information Administration. Average retail price of electricity to ultimate customers. ⟨http://www.eia.gov⟩.
[11] Saied Dardour, Simon Nisan, Françoise Charbit, Utilisation of waste heat from GT–MHR and PBMR reactors for nuclear desalination, Desalin. 205(1) (2007) 254–268.
[12] Mortaza Yari, Waste heat recovery from closed Brayton cycle using organic Rankine cycle: thermodynamic analysis. ASME Turbo Expo 2009: power for Land, Sea, and Air, American Society of Mechanical Engineers, 2009.
[13] Mortaza Yari, S.M.S. Mahmoudi, Utilization of waste heat from GT-MHR for power generation in organic Rankine cycles, Appl. Therm. Eng. 30(4) (2010) 366–375.
[14] Mortaza Yari, S.M.S. Mahmoudi, A thermodynamic study of waste heat recovery from GT-MHR using organic Rankine cycles, Heat Mass Transf. 47(2) (2011) 181–196.
[15] Paola Bombarda, Costante M. Invernizzi, Claudio Pietra, Heat recovery from Diesel engines: a thermodynamic comparison between Kalina and ORC cycles, Appl. Therm. Eng. 30(2) (2010) 212–219.
[16] Daniël Walraven, Ben Laenen, William D'haeseleer, Comparison of thermodynamic cycles for power production from low-temperature geothermal heat sources, Energy Convers. Manag. 66 (2013) 220–233.
[17] Zhenhua Kang, et al., Parametric optimization and performance analysis of zeotropic mixtures for an organic Rankine cycle driven by low-medium temperature geothermal fluids, Appl. Therm. Eng. 89 (2015) 323–331.
[18] Jovana Radulovic, Nadia I. Beleno Castaneda, On the potential of zeotropic mixtures in supercritical ORC powered by geothermal energy source, Energy Convers. Manag. 88 (2014) 365–371.
[19] Bo-Tau Liu, Kuo-Hsiang Chien, Chi-Chuan Wang, Effect of working fluids on organic Rankine cycle for waste heat recovery, Energy 29(8) (2004) 1207–1217.
[20] Chen Yue, et al., Thermal matching performance of a geothermal ORC system using zeotropic working fluids, Renew. Energy 80 (2015) 746–754.
[21] Thoranis Deethayat, Tanongkiat Kiatsiriroat, Chakkraphan Thawonngamyingsakul, Performance analysis of an organic Rankine cycle with internal heat exchanger having zeotropic working fluid case, Stud. Therm. Eng. 6 (2015) 155–161.
[22] Tony Ho, Samuel S. Mao, Ralph Greif, Increased power production through enhancements to the Organic Flash Cycle (OFC), Energy 45(1) (2012) 686–695.
[23] Ngoc Anh Lai, Johann Fischer, Efficiencies of power flash cycles, Energy 44(1) (2012) 1017–1027.
[24] Johann Fischer, Comparison of trilateral cycles and organic Rankine cycles, Energy 36(10) (2011) 6208–6219.
[25] Pedro J. Mago, et al., An examination of regenerative organic Rankine cycles using dry fluids, Appl. Therm. Eng. 28(8) (2008) 998–1007.
[26] Maoqing Li, et al., Construction and preliminary test of a low-temperature regenerative Organic Rankine Cycle (ORC) using R123, Renew. Energy 57 (2013) 216–222.
[27] J.L. Wang, L. Zhao, X.D. Wang, An experimental study on the recuperative low temperature solar Rankine cycle using R245fa, Appl. Energy 94 (2012) 34–40.
[28] A. Soroureddin, et al., Thermodynamic analysis of employing ejector and organic Rankine cycles for GT-MHR waste heat utilization: a comparative study, Energy Convers. Manag. 67 (2013) 125–137.
[29] Naser Shokati, Faramarz Ranjbar, Mortaza Yari, Comparative and parametric study of double flash and single flash/ORC combined cycles based on exergoeconomic criteria, Appl. Therm. Eng. 91 (2015) 479–495.
[30] A. Kalina, Generation of energy by means of a working fluid, and regeneration of a working fluid. U.S. Patent No. 4,346,561. 31 Aug, 1982.
[31] H.D. Madhawa Hettiarachchi, et al., The performance of the Kalina cycle system 11 (KCS-11) with low-temperature heat sources, J. Energy Resour. Technol. 129(3) (2007) 243–247.
[32] Rama Usvika, Maulana Rifaldi, Agus Noor, Energy and exergy analysis of kalina cycle system (KCS) 34 with mass fraction ammonia-water mixture variation, J. Mech. Sci. Technol. 23(7) (2009) 1871–1876.
[33] Xinxin Zhang, Maogang He, Ying Zhang, A review of research on the Kalina cycle, Renew. Sustain. Energy Rev. 16(7) (2012) 5309–5318.
[34] V. Zare, S.M.S. Mahmoudi, M. Yari, Ammonia–water cogeneration cycle for utilizing waste heat from the GT-MHR plant, Appl. Therm. Eng. 48 (2012) 176–185.
[35] M. Fallah, et al., Advanced exergy analysis of the Kalina cycle applied for low temperature enhanced geothermal system, Energy Convers. Manag. 108 (2016) 190–201.
[36] M. Yari, et al., Exergoeconomic comparison of TLC (trilateral Rankine cycle), ORC (organic Rankine cycle) and Kalina cycle using a low grade heat source, Energy 83 (2015) 712–722.
[37] Carlos Eymel Campos Rodríguez, et al., Exergetic and economic comparison of ORC and Kalina cycle for low temperature enhanced geothermal system in Brazil, Appl. Therm. Eng. 52(1) (2013) 109–119.
[38] A. Nemati, V. Fathi, R. Barzegar, S. Khalilarya, Numerical investigation of the effect of injection timing under various equivalence ratios on energy and exergy terms in a direct injection SI hydrogen fueled engine, Int. J. Hydrog. Energy 38 (2) (2013) 1189–1199.
[39] A. Nemati, H. Nami, M. Yari, F. Ranjbar, H.R. Kolvir, Development of an exergoeconomic model for analysis and multi-objective optimization of a thermoelectric heat pump, Energy Convers. Manag. 130 (2016) 1–3.
[40] Kirtipal A. Barse, Michael D. Mann, Maximizing ORC performance with optimal match of working fluid with system design, Appl. Therm. Eng. 100 (2016) 11–19.

[41] Y.M. Kim, C.G. Kim, D. Favrat, Transcritical or supercritical CO 2 cycles using both low-and high-temperature heat sources, Energy 43(1) (2012) 402–415.
[42] S.A. Klein, Engineering equation solver (EES), F-Chart Software, 2006.
[43] H. Nami, F. Ranjbar, M. Yari, S. Saeidi, Thermodynamic analysis of a modified oxy-fuel cycle, high steam content Graz cycle with a dual-pressure heat recovery steam generator', Int. J. Exergy 21 (3) (2016) 331–346.
[44] H. Nami, S.M. Mahmoudi, A. Nemati, Exergy, economic and environmental impact assessment and optimization of a novel cogeneration system including a gas turbine, a supercritical CO 2 and an organic Rankine cycle (GT-HRSG/SCO 2), Appl. Therm. Eng. 110 (2017) 1315–1330.
[45] M. Sadeghi, A. Nemati, M. Yari, Thermodynamic analysis and multi-objective optimization of various ORC (organic Rankine cycle) configurations using zeotropic mixtures, Energy 109 (2016) 791–802.
[46] H. Nami, F. Mohammadkhani, F. Ranjbar, Utilization of waste heat from GTMHR for hydrogen generation via combination of organic Rankine cycles and PEM electrolysis, Energy Convers. Manag. 127 (2016) 589–598.
[47] A. Nemati, R. Barzegar, S. Khalilarya, The effects of injected fuel temperature on exergy balance under the various operating loads in a DI diesel engine, Int. J. Exergy 17 (1) (2015) 35–53.
[48] S. Saeidi, S.M. Mahmoudi, H. Nami, M. Yari, Energy and exergy analyses of a novel near zero emission plant: combination of MATIANT cycle with gasification unit, Appl. Therm. Eng. 108 (2016) 893–904.
[49] A. Nemati, R. Barzegar, S.K. Arya, H. Khatamnezhad, Decreasing the emissions of a partially premixed gasoline fueled compression ignition engine by means of injection characteristics and exhaust gas recirculation, Therm. Sci. 15 (4) (2011) 939–952.
[50] H.M. Hettiarachchi, M. Golubovic, W.M. Worek, Y. Ikegami, The performance of the Kalina cycle system 11 (KCS-11) with low-temperature heat sources, J. Energy Resour. Technol. 129 (3) (2007) 243–247.
[51] S. Ogriseck, Integration of Kalina cycle in a combined heat and power plant, a case study, Appl. Therm. Eng. 29 (14) (2009) 2843–2848.
[52] M. Yari, Exergetic analysis of various types of geothermal power plants, Renew. Energy 35 (1) (2010) 112–121.
[53] V. Zare, S.M. Mahmoudi, A thermodynamic comparison between organic Rankine and Kalina cycles for waste heat recovery from the gas turbine-modular helium reactor, Energy 79 (2015) 398–406.
[54] T.G. Kolda, R.M. Lewis, V. Torczon, Optimization by direct search: new perspectives on some classical and modern methods, SIAM Rev. 45 (3) (2003) 385–482.
[55] R. Senthil Murugan, P.M.V. Subbarao, Effective utilization of low-grade steam in an ammonia—water cycle, Proc. Inst. Mech. Eng. A: J. Power Energy 222. 2 (2008) 161–166.